A THEORETICAL INVESTIGATION INTO THE EFFECT OF A HOMOGENEOUS CATALYST ON COMBUSTION CHARACTERISTICS OF SINGLE DROPLETS OF DIESEL AND BIODIESEL

Mingming Zhu[1*], Yu Ma[1] and Dongke Zhang[1]

[1]Centre for Energy (M473)
The University of Western Australia
35 Stirling Highway, Crawley, WA 6009
* Zhum03@mech.uwa.edu.au

ABSTRACT

The primary objective of this study is to investigate the effect of a ferrous picrate based catalyst on combustion characteristics of single droplets of diesel and biodiesel through mathematical modelling. The ferrous picrate based catalyst was doped into diesel and biodiesel and the single droplets were suspended at the tip of a quartz fibre undergoing heating, ignition and subsequent combustion in a hot stagnation environment. A comprehensive mathematical model was formulated incorporating the effects of fibre conduction, liquid-phase conduction, gas phase reaction and flame radiation. The model was solved by assuming a quasi-steady combustion process and uniform and constant atmospheric pressure. Methyl oleate was used as model fuel of the biodiesel. For the droplet size variation and burning rate, good agreement was found between the modelling results and experimental data. The model predicted higher burning rates of both diesel and biodiesel droplets with the use of the catalyst, which was mainly attributed to the increased flame temperature. The modelling results showed that the surface temperature of droplets of both diesel and biodiesel reached the decomposition temperature of the ferrous picrate (523K) after ignition. This validated our postulation that the ferrous picrate decomposed during the combustion process of single droplets of diesel and biodiesel to release iron atoms into the flame region, which in turn enhanced the reaction rate and therefore increased the flame temperature.

INTRODUCTION

Ferrous picrate, used as a homogeneous combustion catalyst, has been found to save fuel consumption up to approximately 4.2% and reduce smoke emission up to about 40% based on the authors' laboratory observations (Zhu et al., 2011, Zhu et al., 2012). In order to understand the working mechanisms of the ferrous picrate based catalyst in diesel engines, the combustion characteristics of single droplets of diesel and biodiesel dosed with the catalyst has been studied (Zhu et al., 2011). The droplets were suspended at the tip of a quartz fibre and were ignited in a hot tube furnace. It was found that the catalyst increased flame temperature and enhanced burning rates of droplets. Iron ions were also detected in the flames. It was therefore postulated that the released iron atoms upon the decomposition of the ferrous picrate promoted the gas phase reaction rate and increased the flame temperature (Zhu et al., 2012). The increased flame temperature in turn enhanced the burning rates of droplets and reduced the burnout times.

This paper presents a theoretical analysis of the combustion of single droplets to examine the experimental observations and hypotheses and to determine if it is possible for the ferrous picrate to decompose during the combustion process of the droplets and whether the increased flame temperature is mainly responsible for the increased burning rate. A comprehensive mathematical model was formulated incorporating the effects of fibre conduction, liquid-phase conduction, gas phase reaction and flame radiation. With this model, the predicted burning rate of a droplet of the catalyst treated fuel was compared with the experimentally measured burning rate and the results will help to elucidate the working mechanisms of the catalyst in the combustion process of diesel and biodiesel droplets.

MATHEMATICAL MODEL

The physical problem to be simulated was the ignition and combustion of single droplets in Ref. (Zhu et al., 2012). It is illustrated in Fig. 1.
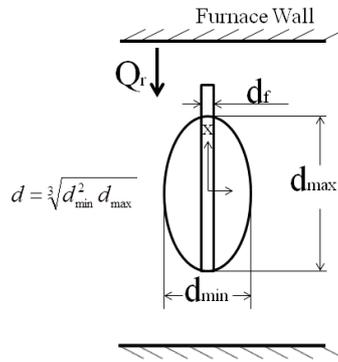

Fig.1 Schematic of the physical problem

The droplet was subjected to the heat radiation from the furnace wall and heat input through the fibre conduction. In the present model, the following assumptions were made (Sazhin, 2006, Yang and Wong, 2001, Shanygan and Prakash, 1995, Chang and Shieh, 1995):

1: The pressure is constant everywhere and the momentum equation is unnecessary;

2: The system is spherically symmetric and one-dimensional;

3: Transport properties are constant along the radial direction based on the reference temperature and composition. The reference temperature was estimated according the following equations (Bergeron and Hallett.William, 1989):

$$T_{ave} = \frac{2}{3}T_s + \frac{1}{3}T_\infty \tag{1}$$

$$Y_{ave} = \frac{2}{3}Y_s + \frac{1}{3}Y_\infty \tag{2}$$

4: The chemical reaction in the gas phase is modelled using a single step Arrhenius equation (Westbrook and Dryer, 1981):

$$W_F = K\rho^{m+n}Y_F^m Y_O^n \exp(\frac{-E}{RT}) \tag{3}$$

where K is the pre-exponential factor and E is the activation energy. In the current calculation, $E = 87\,KJ/mole$, $m = 0.25$ and $n = 1.5$;

2

5: Heat input through the fibre is evenly distributed within the droplet volume (Yang and Wong, 2001);

6: The gas phase reaction is quasi-steady (Bergeron and Hallett.William, 1989);

7: The catalyst has no effect on the transportation properties and thermodynamic data of the gas and liquid. The catalyst only affects the flame temperature;

8: Methyl oleate was used as a model fuel of the biodiesel (Golovitchev and Yang, 2009).

Governing Equations

Gas phase:

The conservation equations in gas phase:

$$\rho C_p \frac{\partial T}{\partial t} + \frac{1}{r^2}\frac{d}{dr}(\lambda r^2 \frac{dT}{dr}) - \rho v C_p \frac{dT}{dr} + W_F Q_F = 0 \tag{4}$$

$$\frac{1}{r^2}\frac{d}{dr}(D\rho r^2 \frac{dY_i}{dr}) - \rho v C_p \frac{dY_i}{dr} + W_i = 0 \quad i = F, O \tag{5}$$

$$G = 4\pi r_p^2 \rho v \tag{6}$$

Liquid Phase:

$$\rho_L C_{PL} \frac{\partial T_l}{\partial t} = \frac{1}{r^2}(\kappa_l r^2 \frac{\partial T_l}{\partial r}) + \dot{Q}_f \tag{7}$$

$$G_S = [-\frac{D\rho}{1-Y_{FS}}]\frac{\partial Y_F}{\partial r}\Big|_s \tag{8}$$

The energy balance at the interface:

Initial Conditions:

At $t = 0$

$$r \le R(t): T_l = T_0 \tag{9}$$

$$r > R(t): T_g = T_\infty, Y_{F,g} = 0 \tag{10}$$

Boundary conditions:

(a) At the droplet centre ($r = 0$):

$$\frac{\partial T_l}{\partial r} = 0 \tag{11}$$

(b) At the droplet surface ($r = R(t)$)

$$T = T_S, Y_F = Y_{FS}, Y_O = Y_{OS} = 1 - Y_{NS} - Y_{FS} \tag{12}$$

Thermodynamic equilibrium relation between T_S and Y_{FS} is evaluated using the Clausius-Clapeyron equation:

$$Y_{FS} = [1 + (\frac{P}{P_S} - 1)\frac{M_g}{M_F}]^{-1} \tag{13}$$

where P_s was calculated by the equation in Appendix A.

$$\kappa_l \left.\frac{\partial T_l}{\partial r}\right|_{r=R} = \frac{Nu \cdot \kappa_g}{2 \cdot R}(T_\infty - T_S) + \varepsilon\sigma(T_\infty^4 - T_S^4) - G_s L \tag{14}$$

The ambient temperature T_∞ is the furnace temperature before the ignition and was set to the measured flame temperature after the ignition. L is the latent heat.

$$Nu = 2 + 0.6\,\mathrm{Re}^{1/2}\,\mathrm{Pr}^{1/3} \tag{15}$$

$$\mathrm{Re} = 2r_s v_d / \upsilon_g \tag{16}$$

$$\mathrm{Pr} = c_{pg}\mu_g / k_g \tag{17}$$

$$\dot{R} = \frac{dR}{dt} = -\frac{G_S}{\rho_L} \tag{18}$$

(c) At infinity ($r \rightarrow \infty$)

$$T = T_\infty,\ Y_F = Y_{F\infty} = 0,\ Y_O = Y_{OS} = 1 - Y_{NS} - Y_{FS} = 0.21 \tag{19}$$

Calculation of fibre conduction input $Q_f(t)$

To calculate the conduction heat input through the fibre, a transient one-dimensional analysis was used, described as follows (Yang and Wong, 2001).

Because the fibre in fine and the Biot number is of the order $O(10^{-2})$ (Yang and Wong, 2001), the temperature distribution in the fibre is assumed to be one-dimensional. Neglecting the absorption of the incident radiation by the fibre, the conservation of energy can be written as:

$$\rho_f c_{p,f}\frac{\partial T_f}{\partial t} = k_f\frac{\partial^2 T_f}{\partial x^2} + \frac{4h_\infty}{d_f}(T_\infty - T_f) \tag{20}$$

In the above equation, h_∞, the heat convection coefficient over a horizontal cylinder, is obtained with:

$$h_\infty = Nu_\infty k_\infty / d_f \tag{21}$$

where $Nu_\infty = 0.36$ for the limiting stagnant situation.

Initial condition:

$$T_f(0, x) = T_0 \tag{22}$$

Boundary conditions:

$$\frac{\partial T_f}{\partial x} = 0 \text{ at both } x \rightarrow \infty \text{ and } x \rightarrow 0 \tag{23}$$

The properties of quartz, the fibre material for the current experimentation, are $\rho_f = 2220\,kgm^{-3}$, $k_f = 1.4\,Jm^{-1}s^{-1}K^{-1}$ and $c_{p,f} = 744\,JKg^{-1}$

2

The fibre conduction input can be calculated once T_f is known:

$$\overset{*}{Q}_f = (\int_{-R}^{R} h_\infty (T_\infty - T_f)\pi d_f \, d_x)/V_{net} \qquad (24)$$

where V_{net} is the net volume of the liquid fuel.

Fuel Thermo-Physical Properties

The physical properties of fuel play a pivotal role in determining the accuracy of the results predicted by the mathematical models. Key physical properties including density, vapour pressure, latent heat of vaporisation, specific heat capacity were calculated based on the equations in Appendix A.

Numerical Method

To account for the droplet surface regression during evaporation and combustion, transformations of the spatial coordinates in both liquid and gas phases were made to fix the surface using the following mathematic method:

$$\varepsilon(r,t) = r/R(t) \qquad (25)$$

The fully implicit scheme backward in time and central in space is used to discretise the governing equations and boundary conditions. In our numerical solutions, time step $\Delta t = 1ms$ and grid size $\Delta \varepsilon = 0.01$ are adequately small for all of our computations. Infinity was set at 100 times of the droplet radius.

RESULTS AND DISCUSSION

Model Validation

The theoretical results of the burnout times of droplets of diesel and biodiesel are compared with the experimental data (Zhu et al., 2012) under different ambient temperatures in Fig. 2. Taking the experimental errors into consideration, it is manifested that the agreement between the modelling results and the experimental data was excellent under the conditions studied.
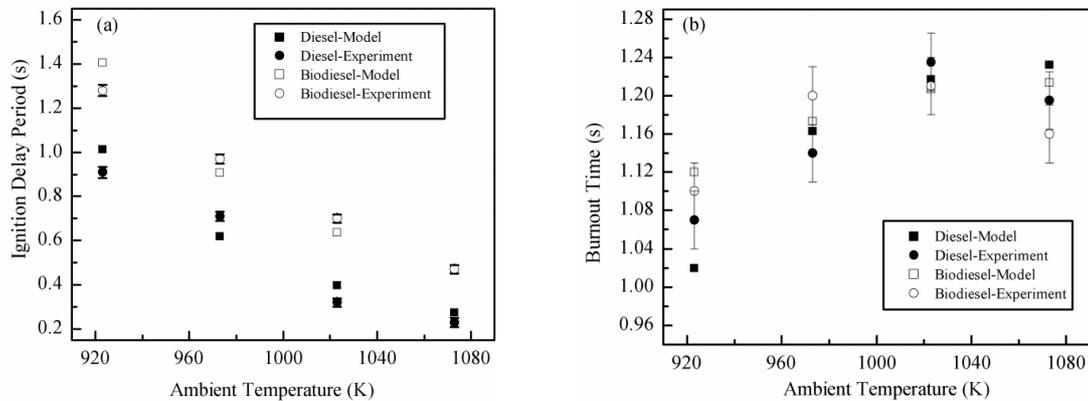

Fig. 2 Comparisons of the experimental data and theoretical results of the ignition delay period and burnout time of diesel and biodiesel droplets at various ambient temperatures

The good agreement between the experimental data and theoretical results, shown in Fig. 2, demonstrates that the current model was reliable enough to capture the main ignition and combustion characteristics of the single droplets of diesel and biodiesel. The deviations between the experimental data and the modelling results could be accounted for by the fact that few real physical phenomena were simplified in the current model. The gas phase reaction was modelled using one step Arrhenius equation, which was not sufficient enough to simulate the real complex chemical reactions of diesel and biodiesel fuel burning in the hot air. Furthermore, the soot radiation was also simplified in the current model, neglecting the specific soot formation mechanisms and soot radiation characteristics.

Effect of the Catalyst

The theoretical results of the time variation of the squared droplet diameter after ignition for both diesel and biodiesel are shown in Fig. 3 and compared with the experimental data (Zhu et al., 2012). In each plot, the calculations with and without the effects of the catalyst were included.
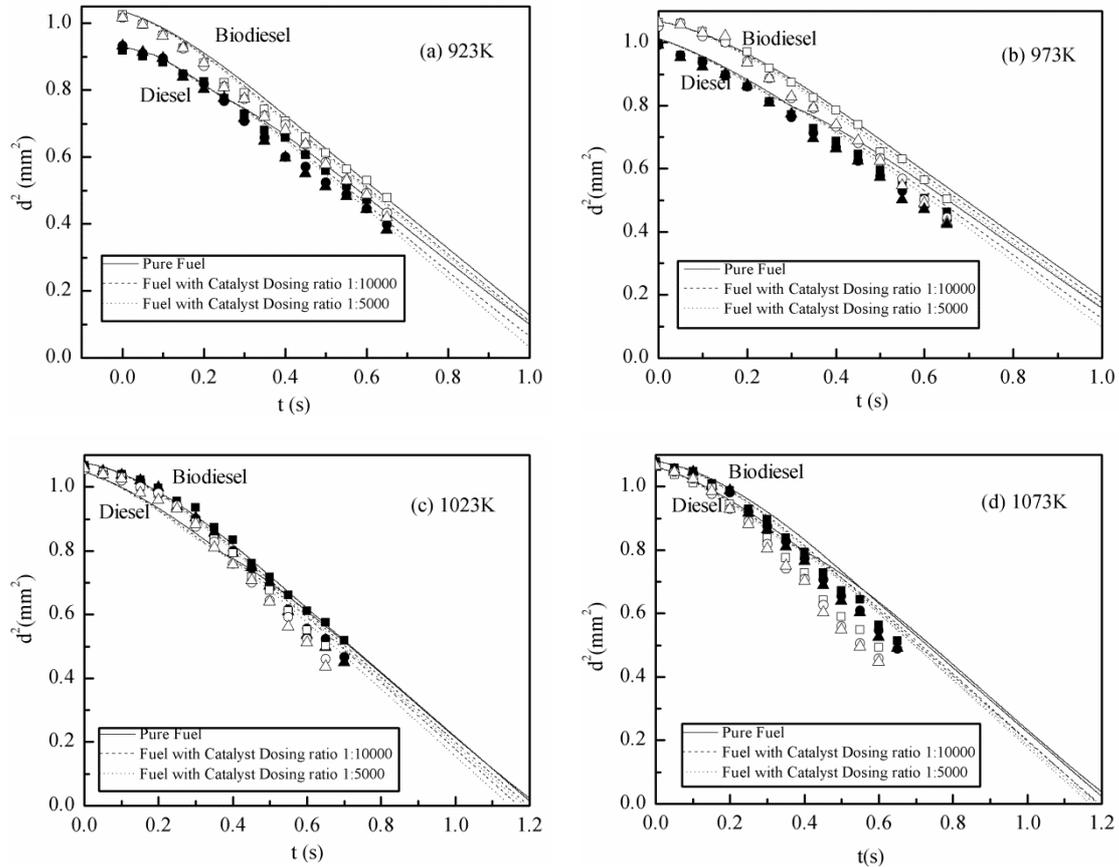

Fig. 3 Theoretical and experimental time variations of squared droplets diameter of diesel and biodiesel with different catalyst dosing ratio at different ambient temperatures (Experimental symbols ■:diesel;●:diesel dosed with the catalyst at a dosing ratio of 1:10000;▲: diesel dosed with the catalyst at a dosing ratio of 1:5000;□ :biodiesel;○:biodiesel dosed with the catalyst at a dosing ratio of 1:10000;△:biodiesel dosed with the catalyst at a dosing ratio of 1:5000)

Both theoretical and experimental results show that the square of the droplet diameter decreased with the time, but was not linearly until after a short period. The well established d^2-law (Dietrich et al., 1996, Faeth, 1977, Law, 1982) dictates that the square of the droplet diameter decreases linearly with time. However, for the big droplets used in the current experimentation, the d^2-law is only well conformed to by the burning droplets after an initial period of heating. It is evident from the theoretical results that the square of the droplet diameter tended to decrease in a faster manner with the addition of the catalyst in the fuels due to the increased flame temperature.

Fig. 4 shows the theoretical burning rates of droplets of diesel and biodiesel with the catalyst at different ambient temperatures. The experimental burning rates were also included for comparisons. For both of the theoretical and experimental results, the burning rate was determined as $K = -d(d_s^2)/dt$ based on the data after the $d^2/d_0^2 = 0.5$ (Yang and Wong, 2001). Considering the experimental errors, it is seen that the theoretical and experimental data matched each other very well, in which the use of the catalyst enhanced the burning rates of both fuels. As the catalyst only affected the flame temperature assumed in this model, the good agreement between the experimental and modelling results implies that the increased burning rate with the use of the catalyst was mainly attributed to the increased flame temperature.
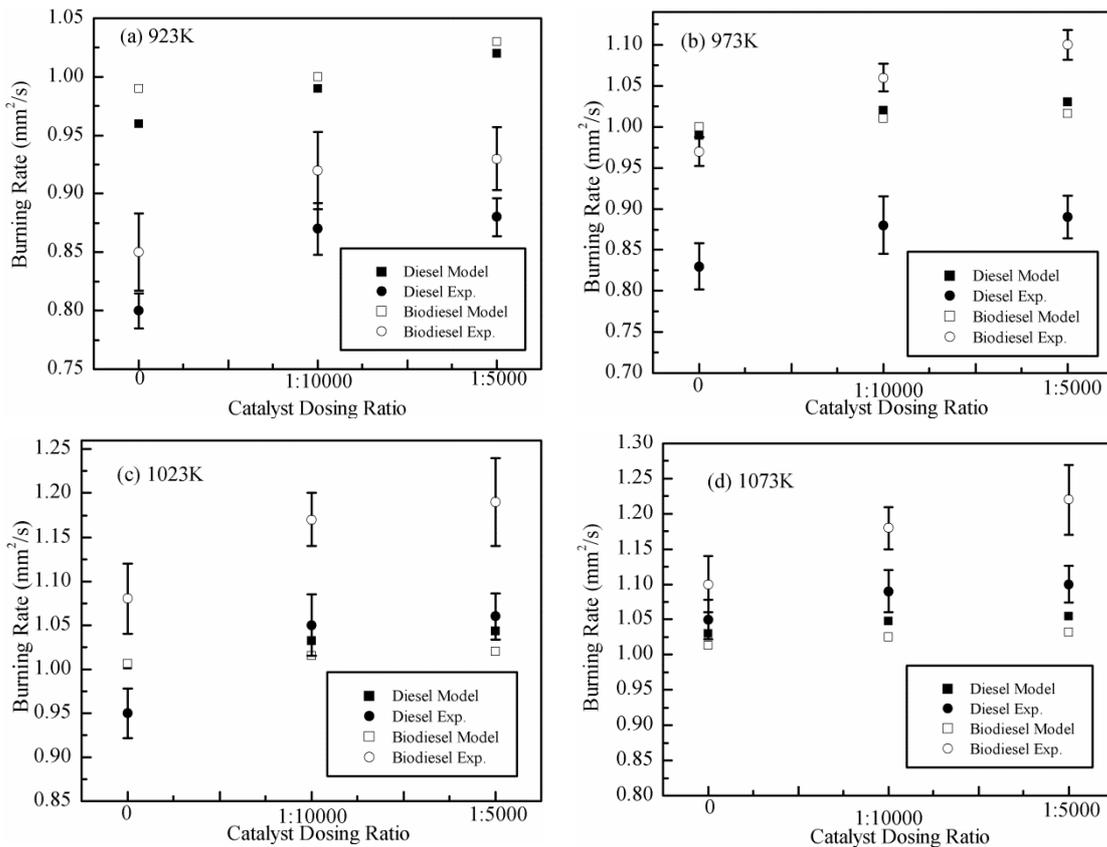

Fig. 4 Theoretical and experimental burning rates of diesel and biodiesel with different catalyst dosing ratio at different ambient temperatures

In our previous experimental work, it was observed that the ferrous picrate decomposed at the temperature around 523K (Zhu et al., 2012). The decomposed iron atom was released into the flame, which was postulated to catalyse the gas phase reaction and accelerated the reaction rate. Fig. 5 shows the surface temperature of droplets of diesel and biodiesel at air temperature of 973K. It is seen that droplet surface temperatures

were below the boiling points of both fuels before the ignition point. After the ignition, the surface temperature continued to rise and reached the boiling point in a short period, which corresponds to the heating period shown in the Fig. 3 after the ignition point. It is also seen that both boiling points of diesel and biodiesel was higher than the decomposition temperature of the ferrous picrate, which implies that it is certain that the ferrous picrate decomposed after the ignition when it was exposed to a reacting gas environment with temperature equal or higher than its decomposition temperature and released the iron atoms into the flame.
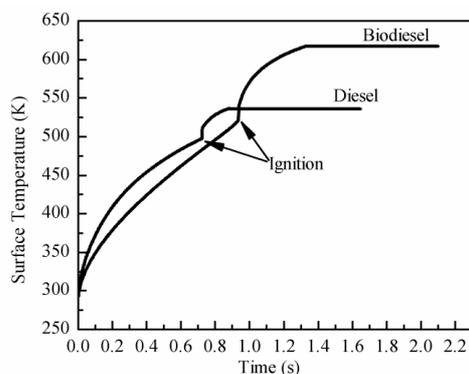

Fig. 5 Surface temperatures of droplets of diesel and biodiesel at air temperature of 973K

CONCLUSIONS

A detailed mathematical model has been developed to account for the effect of a ferrous picrate based catalyst on the ignition and combustion characteristics of single droplets of diesel and biodiesel suspended at the tip of a quartz fibre undergoing heating, ignition and subsequent combustion in a hot stagnation environment. The formulated model incorporated the effects of fibre heat conduction, liquid-phase conduction, gas phase reaction and flame radiation. The model was validated by the corresponding experimental work and a good agreement has been achieved at various ambient temperatures in terms of the ignition delay period and burnout time.

The model predicted higher burning rates of both diesel and biodiesel droplets with the use of the catalyst, which is attributed to the increased flame temperature. The modelling results showed that the surface temperatures of droplets of both diesel and biodiesel reached the decomposition temperature of the ferrous picrate (523K) after ignition. This validated our postulation that the ferrous picrate decomposed during the combustion process of single droplets of diesel and biodiesel to release iron atoms into the flame region, which in turn enhanced the gas phase reaction rate and therefore increased the flame temperature.

ACKNOWLEDGEMENT

APPENDIX A. KEY PHYSICAL PROPERTIES OF FUELS

Vapour pressure

The vapour pressure for diesel (Sazhin, 2006, Chin and Lefebvre, 1985):

$$P_s = \begin{cases} 1000 \times \exp[8.5872101 - 2591.5232/(T-43)], T < 380K \\ 1000 \times \exp[14.060729 - 4436.099/(T-43)], 380 \leq T < 500K \\ 1000 \times \exp[12.93692 - 3922.5184/(T-43)], 500 \leq T < 620K \\ 1000 \times \exp[16.209535 - 5810.817/(T-43)], 620 \leq T < T_{cr} \\ 0, T \geq T_{cr} \end{cases}$$

The vapour pressure for biodiesel using Antoine equation (J.A.Riddick et al., 1986):

$$P_s = 1000 \times 10 \wedge [6.0054 - 1963.525/(T-142)], T \leq T_{cr}$$

T_{cr} is the critical temperature of fuels; $T_{cr} = 726K$ for diesel (Sazhin, 2006) and $T_{cr} = 764K$ for biodiesel (J.A.Riddick et al., 1986)

Density

The Racket equation modified by Spencer and Danner (Reid et al., 1987) was employed to predict the liquid density:

$$\rho = 0.84 * 0.2499^{-\varphi} \text{ for diesel and } \rho = 0.87 * 0.2370^{-\varphi} \text{ for biodiesel}$$

$$\varphi = (1 - T/T_{cr})^{2/7} - (1 - 273.15/T_{cr})^{2/7}$$

Latent heat of vaporisation

The latent heat of vaporisation of the liquid was determined using the equation proposed in (Chin and Lefebvre, 1985):

$$L = 254000((T_{cr} - T)/(T_{cr} - T))^{0.38} \text{ for diesel}$$

$$L = 238000((T_{cr} - T)/(T_{cr} - T))^{0.38} \text{ for biodiesel}$$

Specific Heat Capacity

Bondi's modification of Rowlinson's method (Reid et al., 1987) was used to estimate the specific heat capacity of the liquid as a function of temperature:

$$\frac{C_l - C_l^0}{R} = 2.56 + 0.436(1 - T_r)^{-1} + \omega[2.91 + 4.28(1 - T_r)^{0.33} T_r^{-1} + 0.296(1 - T_r)^{-1}]$$

$$\alpha = -\ln P_c - 5.97214 + 6.09648\theta^{-1} + 128862\ln\theta - 0.169347\theta^6$$

$$\beta = 15.2518 - 15.6875\theta^{-1} - 13.4721\ln\theta + 0.43577\theta^6$$

where $\omega = \alpha/\beta$, $T_r = T/T_{cr}$, $\theta = T_b/T_{cr}$ and C_l^0 is the specific heat capacity at reference state (273.15K, 1atm) J/mole⁻¹K⁻¹. T_b is the boiling point of fuels. $T_b = 536K$ for diesel and $T_b = 617K$ for biodiesel.

NOMENCLATURES

$R(t)$	droplet radius	ρ	density
C_p	constant-pressure specific heat	*Subscripts*	
k	thermal conductivity	∞	environment
M	molecular weight	F	fuel
Y	mass fraction	g	gas phase
r	spatial coordinate	l	liquid phase
P	pressure	f	support fibre
T	temperature	0	initial state
Greek symbols		s	surface
ε	emissivity	cr	critical point
σ	Stefan-Boltzmann constant	b	boiling point

REFERENCES

BERGERON, C. A. & HALLETT.WILLIAM, L. H. 1989. Ignition characteristics of liquid hydrocarbon fuel as single droplets. *The Canadian Journal of Chemical Engineering,* 67.

WESTBROOK, C.K. & DRYER, F. L. 1981. Simplified reaction mechanisms for the oxidation of hydrocarbon fuels in flames. *Combust.Sci. and Tech.,* 27**,** 31-43.

CHANG, K. C. & SHIEH, J. S. 1995. Theoretical investigation of transient droplet combustion by considering flame radiation. *Int.J.Heat Mass Transfer,* 38**,** 2611-2621.

CHIN, J. S. & LEFEBVRE, A. H. 1985. The role of the heat-up period in fuel drop evaporation. *Int J Turbo Jet Eng,* 2**,** 315-325.

DIETRICH.D.L., J.B.HAGGARD., F.L.DRYER., V.NAYAGAM., B.D.SHOW & F.A.WILLIAMS 1996. Droplet combustion expereiments in spacelab. *Twenty-Sixth Symposium (International) on Combustion***,** 1201-1207.

FAETH, G. M. 1977. Current status of droplet and liquid combusiton. *Prog. Energy Combust. Sci.,* 3**,** 191-224.

GOLOVITCHEV, V. I. & YANG, J. 2009. Construction of combustion models for rapeseed methyl ester bio-diesel fuel for internal combustion engine applications. *Biotechnol Adv,* 27**,** 641-55.

J.A.RIDDICK, BUNGER, W. B. & SAKANO, T. K. 1986. *Organic solvents:physical properties and methods of purification,* New York, Wiley Interscience.

LAW, C. K. 1982. Recent advances in droplet vaporization and combustion. *Prog. Energy Combust. Sci.,* 8**,** 171-201.

REID, R. C., PRAUSNITZ, M. J. & SHERWOOD, T. K. 1987. *The properties of gases and liquids,* New York, McGraw-Hill.

SAZHIN, S. S. 2006. Advanced models of fuel droplet heating and evaporation. *Prog. Energy Combust. Sci.,* 32**,** 162-214.

SHANYGAN, N. & PRAKASH, S. 1995. Droplet ignition and combustion including liquid pahse heating. *Combustion and Flame,* 102**,** 1-10.

YANG, J. R. & WONG, S. C. 2001. On the discrepancies between theretical and experimental results for microgravity droplet evaporation. *Int.J.Heat Mass Transfer,* 44.

ZHU, M., MA, Y. & ZHANG, D. K. 2011. An experimental study of the effect of a homogeneous combustion catalyst on fuel consumption and smoke emission in a diesel engine. *Energy,* 36**,** 6004-6009.

ZHU, M., MA, Y. & ZHANG, D. K. 2012. Effect of a homogeneous combustion catalyst on the combustion characteristics and fuel efficiency in a diesel engine. *Applied Energy,* 91**,** 166-172.

ZHU, M. M., MA, Y. & ZHANG, D. K. The effect of a homogeneous combustion catalyst on the combustion charateristics of single droplets of diesel and biodiesel. Accepted by the 34th International Combustion Symposium, Jul 29-Aug 3, 2012, Warsaw, Poland.

ZHU, M. M., YU, M. & ZHANG, D.K. Effect of a homogeneous combustion catalyst on the combustion charateristics of single droplets of diesel and biodiesel Proceedings of the Australia Combustion Symposium, Nov 29-Dec 1, 2011, The University of Newcastle.